

# Influence of heated forming tools on corrosion behavior of high strength aluminum alloys

## Einfluss beheizter Umformwerkzeuge auf das Korrosionsverhalten hochfester Aluminiumlegierungen

B. Heider<sup>1</sup>, E. Scharifi<sup>2</sup>, T. Engler<sup>1</sup>, M. Oechsner<sup>1</sup>, K. Steinhoff<sup>2</sup>

In this study forming tools tempered at 24 °C and 350 °C were used to systematically investigate the influence of different cooling rates on the mechanical and corrosion properties of a high strength aluminum alloy AA7075 within a novel thermo-mechanical process that combines forming and quenching simultaneously. The samples formed within heated tools reveal higher ductility and lower material strength compared to the parts processed in cold tools. In addition, the corrosion behavior changed between samples formed with 24 °C forming tools and 350 °C forming tools, respectively. Through cyclic polarization in chloride containing aqueous media a change in the hysteresis and shift of open circuit potential was observed. Metallographic investigation revealed that there was also a very different corrosion morphology for the samples formed within the heated tools. No change in average grain size could be detected but changes of the microstructure in sub-grain scale that occur during the forming within the heated tools are responsible for this effect. In further research, the effect of various cooling rates on mechanical and corrosion behavior and the microstructure will be investigated by variation of the forming tool temperature.


**Keywords:** Aluminum alloys / press forming / ultimate stress / total strain / corrosion behavior

Die Einflüsse der Temperatur von Umformwerkzeugen bei 24 °C bzw. 350 °C zur Kontrolle der Abkühlgeschwindigkeit bei einem innovativen Ansatz der Warmumformung der Aluminiumlegierung AA7075 auf mechanische Eigenschaften und das Korrosionsverhalten wurden systematisch untersucht. Durch erwärmte Umformwerkzeuge konnte erhöhte Duktilität bei verringerter Zugfestigkeit dieser Proben im Vergleich zu in kalten Werkzeugen umgeformten Proben erzielt werden. Zusätzlich konnte eine Veränderung des Korrosionsverhaltens zwischen den bei unterschiedlichen Werkzeugtemperaturen umgeformten Proben festgestellt werden. Mittels zyklischen potenziodynamischen Polarisationsmessungen in chloridhaltigem Medium wurden unterschiedliche Verläufe der Hystereseschleifen und Verschiebungen des freien Korrosionspotenzials ermittelt. Gestützt durch metallo-

<sup>1</sup> Zentrum für Konstruktionswerkstoffe (MPA-IfW Darmstadt), TU Darmstadt, Grafenstraße 2, 64283 DARMSTADT, FEDERAL REPUBLIC OF GERMANY

<sup>2</sup> Institut für Produktionstechnik und Logistik, Umformtechnik, Universität Kassel, Kurt-Wolters-Straße 3, 34125 KASSEL, FEDERAL REPUBLIC OF GERMANY

Corresponding author: B. Heider, Zentrum für Konstruktionswerkstoffe (MPA-IfW Darmstadt), TU Darmstadt, Grafenstraße 2, 64283 DARMSTADT, FEDERAL REPUBLIC OF GERMANY, E-Mail: heider@mpa-ifw.tu-darmstadt.de

 This is an open access article under the terms of the Creative Commons Attribution License, which permits use, distribution and reproduction in any medium, provided the original work is properly cited.

grafische Untersuchungen wurden danach unterschiedliche Korrosionsmorphologien bei sonst gleichen mittleren Korngrößen dokumentiert. Diese Beobachtungen sind durch Änderungen im Gefüge auf Subkornebene durch die verzögerte Abkühlung während der Umformung bei 350 °C zu erklären. Der Einfluss verschiedener Abkühlraten auf das Gefüge, die mechanischen Eigenschaften und das Korrosionsverhalten sind Gegenstand weiterer Forschung.

**Schlüsselwörter:** Aluminiumlegierungen / Pressformen / Zugfestigkeit / Bruchdehnung / Korrosionsverhalten

## 1 Introduction

The demand for lightweight structures for reasons of efficiency and sustainability has been increasing throughout the past decades. For this reason, many research efforts aimed towards either increasing the strength of parts, which allows using less of that material or materials with higher strength to weight ratio [1]. An approach to optimize the efficiency of the production process of lightweight structures lies within optimizing the shape of parts while reducing the manufacturing steps. Sheet metal forming is a technique commonly used in e.g. the automotive industry to produce various chassis parts. Since the cold formability of high strength steels on the one hand and aluminum alloys on the other hand is limited, hot forming has been extensively researched and has found its application in industry [2]. High strength aluminum alloys have shown a high potential of being a suitable material and candidate for vehicle structures. For example, the aluminum alloy AA7075 of composition Al–Zn–Mg–Cu is promising for lightweight application due to its high strength to weight ratio and high maximum strength in T6 condition.

Unfortunately, forming of high strength AA7075 alloy is limited due to its low formability and high springback, especially at room temperature, which confines its broad application field. In order to overcome this barrier, different approaches have been developed in the past to improve the formability and drawability at higher temperatures [3–6]. One promising technique that comprises simultaneous forming and quenching reveals high capability for forming of complex-shaped aluminum parts with a considerable reduction in springback after the forming operation without losing the adjusted properties, e.g. tailored yield strength and ductility [7–10].

There is a selection within the studies on hot forming of various aluminum alloy parts which investigate the influence of cooling rates by applying cold tools compared to forming within heated tools [11–14]. On the one hand, the formability increases greatly with significant reduction in springback after forming. On the other hand, there is a great potential to influence the resulting mechanical properties by controlling the forming tool temperature [11].

Usually, these studies do not consider the influence of hot forming in heated tools on the corrosion behavior of the precipitation hardenable aluminum alloys. While it is clear that both size and distribution of precipitates determine the mechanical properties, they affect the corrosion behavior as well [15]. Especially the aluminum alloys of the 7000 series can suffer - depending on their microstructure - from intergranular corrosion and stress corrosion cracking in their highest strength T6 condition. The chemistry of intermetallic precipitates that form during ageing determines their electrochemical corrosion potential and therefore if they are electrochemically anodic or cathodic to the Al-matrix [16]. The initiation of corrosion is a potential difference between the aluminum matrix and the intermetallic phases, e.g. in 7075 alloys  $Al_7Cu_2Fe$ ,  $Al_3Fe$  and  $Al_2CuMg$  being cathodic and  $MgZn_2$  and  $Mg_2Si$  being anodic compared to the aluminum matrix, respectively [17]. The susceptibility to corrosion, especially the intergranular type, increases through ageing up to T6 condition, which has the maximum strength and hardness. On the one hand, the precipitation and growth of intermetallic phases enhances these mechanical properties, but on the other hand, the corrosion properties and stress corrosion susceptibility are deteriorated by the same mechanism [18, 19]. To significantly reduce the susceptibility to stress corrosion crack-

**Table 1.** Chemical composition of the investigated alloy AA7075.**Tabelle 1.** Chemische Zusammensetzung der untersuchten Legierung AA7075.

Chemical elements	Si	Fe	Cu	Mn	Mg	Cr	Zn	Ti	Al
AA7075 [wt.%]	0.05	0.11	1.7	0.02	2.7	0.19	5.8	0.05	Balance

ing, heat treatment to the T73 condition, also known as over-ageing is usually applied [18]. However, by extended ageing after peak-ageing condition T6, precipitates grow further which leads to reduced maximum strength.

It is known that cold forming prior to heat treatment induces dislocations and vacancies in the lattice, which can lead to accelerated ageing towards the maximum strength T6 condition. Another way is a short term heat treatment before ageing through which a number of precipitates can be gained that grow during the ageing and accelerate the ageing process as well [20].

Therefore, the question arises, if hot forming after solutionizing followed by ageing to T6 condition leads to beneficial precipitate morphology and eventually enhanced corrosion properties without major drawbacks in mechanical properties.

## 2 Materials and experimental details

The experimental investigations in this study were carried out on 1.5 mm thick flat rolled product of precipitation hardenable aluminum alloy AA7075 (Al–Zn–Mg–Cu), *Table 1*. The as-received condition was T6 (solution heat-treated, quenched and artificially aged) with a hardness level of 189 HV5, a yield strength (YS) of 523 MPa and an ultimate tensile strength (UTS) of 577 MPa.

### 2.1 Thermo-mechanical forming route

The process investigated in the present work used a roller hearth furnace for solution heat treatment (SHT) of the material, a manual transfer to the hat-shaped forming tools, a hydraulic press and a furnace for the subsequent artificial ageing treatment.

This study is focused on the effect of different cooling strategies on the mechanical and corrosion behavior of AA7075. For this aim, the material is

solution heat treated at a temperature of 480 °C for 20 min to dissolve the alloying elements inside the Al-matrix, *Table 2*. The heated blanks were formed and quenched for 30 s in forming tools that have been tempered either at 24 °C or at 350 °C. Subsequently, in order to achieve maximum strength all formed parts were aged at 120 °C for 20 h.

### 2.2 Mechanical testing

The mechanical properties of the formed parts were determined using a Hegewald & Peschke tensile testing machine (100 kN). For this purpose, tensile samples were cut by electrical discharge machining to a length of 50 mm and to a width of 12.5 mm in rolling direction (according to ASTM/E8-13a).

### 2.3 Corrosion testing

Cyclic potentiodynamic polarization measurements can provide a considerable amount of information on the corrosion kinetics e. g. open corrosion potential (OCP), passivation potential, passive current density and repassivation behavior. A silver/silver-chloride (Ag/AgCl) electrode is used as a reference and the potentials are given with respect to the standard hydrogen electrode (SHE). A platinum mesh serves as counter electrode while the samples

**Table 2.** Process parameters of the focused thermo-mechanical route for AA7075.**Tabelle 2.** Parameter des thermomechanischen Prozessverlaufes für AA7075.

	SHT temperature	SHT time	Tool temperature	Ageing treatment
1	480 °C	20 min	24 °C	120 °C–20 h.
2	480 °C	20 min	350 °C	120 °C–20 h.

(18 mm × 18 mm × 1.5 mm) are built into a sample holder made of polyether ether ketone (PEEK). A sodium chloride (NaCl) solution with 0.1 % by weight concentration, pH value of approx. 5.6 and conductivity of 2.0 mS/cm is used as test medium. The potentiostat Reference 600 (Gamry Instruments, Warminster, PA, USA) controls the experiment with a sample rate of 1 s: After 15 min of open circuit potential measurement, the potential is increased from  $-0.2 V_{\text{OCP}}$  with a scan rate of 1 V/h and after reaching a maximum current density of  $0.3 \text{ mA/cm}^2$  with the same scan rate the potential is decrease to  $-0.3 V_{\text{OCP}}$ . Three tests are conducted on samples that were ground to 4000 grit finish.

### 3 Results

#### 3.1 Mechanical properties

The solution heat treated, subsequently in forming tools tempered at  $24^\circ\text{C}$  hot formed and at  $120^\circ\text{C}$  for 20 h artificially aged material shows a slight increase in yield (540 MPa) and ultimate tensile strength (591 MPa) compared to the as-received T6-condition (523 MPa yield strength, 577 MPa ultimate tensile strength) and the stress-strain curves from tensile test have a similar shape for both materials, *Figure 1*. After forming at higher tool temperature,  $350^\circ\text{C}$ , the yield strength and ultimate tensile strength decrease dramatically to 156 MPa and 332 MPa, respectively. Thus, hot stamping of AA7075 at lower tool temperature reveals higher material strength, comparable to those of the as-received T6-condition. In case of elongation to failure, an increase of the total strain level with increasing the tool temperature was observed. This behavior and the considerable drop in material strength can be explained by the nucleation and growth of precipitates generated already during the hot forming process. The lower amount of solutes in the matrix after hot forming leads to reduced artificial age hardening effect of this material.

#### 3.2 Corrosion behavior

After the cyclic potentiodynamic polarization test, the surface of the samples that was exposed to the electrolyte looks darker compared to the pristine

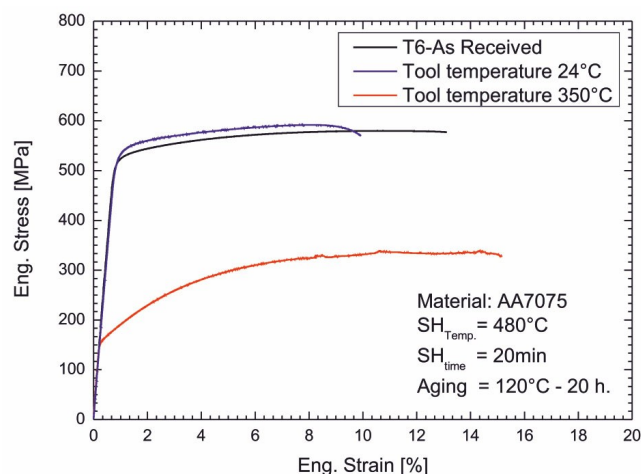


**Figure 1.** Tensile properties of the investigated material AA7075 after forming at different tool temperatures compared to the as-received condition.

**Bild 1.** Spannungs-Dehnungsdiagramm der untersuchten Legierung AA7075 nach Umformung in unterschiedlich temperierten Werkzeugen im Vergleich zum Anlieferungszustand.

surface, *Figure 2*. The discoloration is homogeneous and the borderline is sharp. Visually, there is no clear difference between the test surfaces of the samples that were formed without or with heated forming tools, respectively.

The current density-potential diagrams resulting from cyclic potentiodynamic polarization measurements give information about the corrosion kinetics, i.e. active corrosion or passive behavior, the type of hysteresis at the point of polarization reversing and a shift of the open corrosion potential, *Figures 3, 4*. The data is only displayed until the open circuit po-

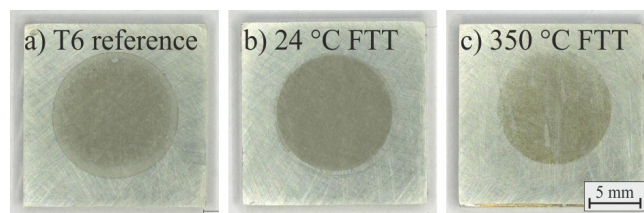


**Figure 2.** Photographs of test surfaces after cyclic potentiodynamic polarization test: a) T6 reference sample and samples formed with b)  $24^\circ\text{C}$  and c)  $350^\circ\text{C}$  forming tool temperature.

**Bild 2.** Dokumentation der Testflächen nach zyklischer potenziodynamischer Polarisation: a) T6 Referenzprobe und die in auf b)  $24^\circ\text{C}$  und c)  $350^\circ\text{C}$  temperierten Werkzeugen umgeformten Proben.

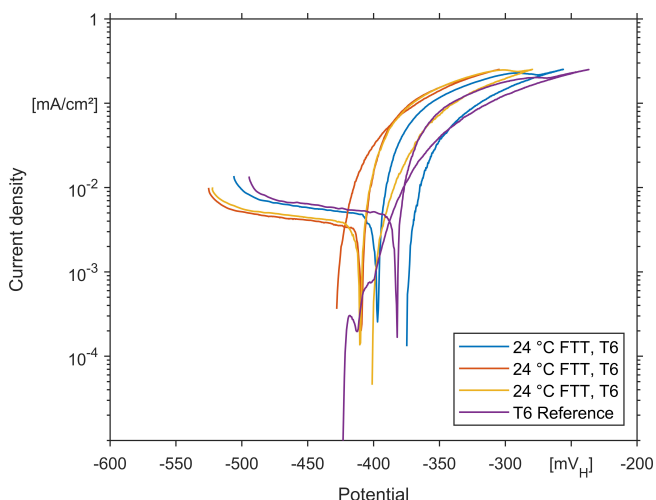


**Figure 3.** Current density-polarization curves of samples formed at 24 °C forming tool temperature (FTT) and T6 reference sample in 0.1 % NaCl solution.

**Bild 3.** Stromdichte-Potenzialkurven der in auf 24 °C temperierten Werkzeugen umgeformten Proben in 0,1 % NaCl-Lösung.

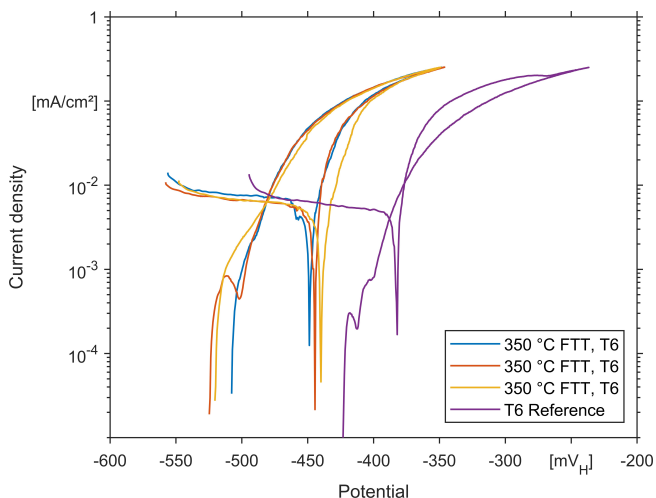


**Figure 4.** Current density-polarization curves of samples formed at 350 °C forming tool temperature (FTT) and T6 reference sample in 0.1 % NaCl solution.

**Bild 4.** Stromdichte-Potenzialkurven der in auf 350 °C temperierten Werkzeugen umgeformten Proben in 0,1 % NaCl-Lösung.

tential is passed on the backward sweep for better differentiation between forward sweep and backward sweep. Average values from each three measurements were extracted from the current density-potential curves, *Table 3*. Initially, the open circuit potential of the T6 reference sample during the forward sweep was the most positive, i.e. the noblest. During the

**Table 3.** Overview of electrochemical parameters (average values of each three measurements) gained from cyclic potentiodynamic polarization measurement in 0.1 % NaCl solution.

**Tabelle 3.** Übersicht der aus den zyklischen potenziodynamischen Polarisationsmessungen in 0,1 % NaCl-Lösung ermittelten elektrochemischen Parameter (Mittelwert aus jeweils drei Messungen).

Sample	OCP forward [mV <sub>H</sub> ]	Hysteresis type	OCP backward [mV <sub>H</sub> ]	ΔOCP [mV]
T6 reference	−384	negative	−420	−36
24 °C FTT	−405	negative	−401	+ 4
350 °C FTT	−444	positive	−518	−74

backward sweep the open circuit potential changed to more negative values for both the T6 reference sample and the sample formed with 350 °C forming tool temperature. For the sample formed with 24 °C forming tool temperature, an average shift towards slightly more positive values during the backward sweep was recorded. There were also differences in the hysteresis type at the point of polarization reversing. On the one hand, the hysteresis type was negative for T6 reference samples (purple) and the samples formed with 24 °C forming tool temperature (2 of 3 tests: blue and yellow curves; red curve backward-sweep is similar to forward-sweep), while on the other hand the hysteresis type was positive for the samples formed with 350 °C forming tool temperature (all curves). The meaning of this positive hysteresis type in this case is most likely that the corrosion continued after the point of polarization reversing, which is underlined by the shift of the open circuit potential towards more negative values, i.e. a deterioration of the surface. The deterioration is documented by the micrographs prepared perpendicular to the original rolling direction, *Figure 5*.

Intergranular and pitting corrosion attacks are found at the surface of the T6 reference sample. At the surface of the sample formed with 24 °C forming tool temperature, light intergranular corrosion attack was documented. The corrosion attack at the surface of the sample formed with 350 °C forming tool temperature was more intense and the largest investigated pit had an extension of approx. 80 μm width and 20 μm depth.

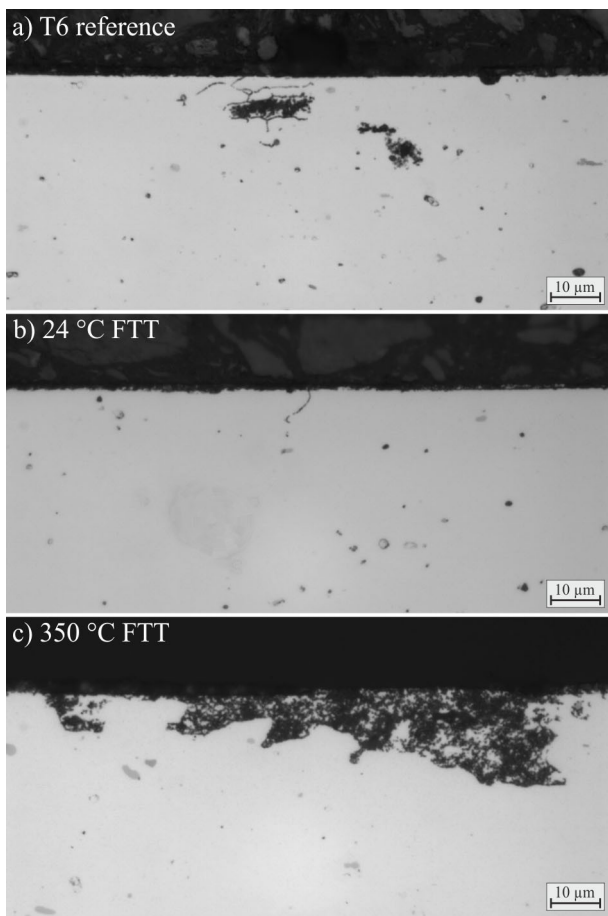


**Figure 5.** Cross-sections of test surfaces after cyclic potentiodynamic polarization test in 0.1 % NaCl solution: a) T6 reference sample and samples formed at b) 24 °C and c) 350 °C forming tool temperature.

**Bild 5.** Querschliffansichten aus dem Bereich der Testflächen der a) T6 Referenzprobe und den in auf b) 24 °C und c) 350 °C temperierten Werkzeugen umgeformten Proben nach zyklischer Polarisation in 0,1 % NaCl-Lösung.

## 4 Discussion

The full age hardening potential is only obtained with a tool temperature of 24 °C due to the high cooling rate which lead to a sufficient supersaturation in the solid solution after forming and quenching. The attained high strength is consequently generated by the formation of fine precipitates during artificial ageing. Forming at higher tool temperatures leads to a retardation of the cooling which results in lower yield and tensile strength but significantly increased elongation at failure. This observation can be explained by the formation and growth of coarse stable phases, which have a little strengthening effect [20].

The material formed at 24 °C forming tool temperature showed different corrosion behavior compared to the samples formed at 350 °C forming tool temperature. While rapid cooling of the samples in the forming tool without heating suppresses formation of nuclei for precipitation, lower cooling rates, higher diffusion rates and longer time for diffusion in the samples in the heated forming tool lead to formation of nuclei and precipitates. Large precipitates grow from these nuclei during the subsequent artificial ageing process. While those larger precipitates contain more alloying elements, the adjacent areas are depleted of those elements. This chemical gradient is in turn reflected as a gradient in electrochemical potential, which can cause the initiation of corrosion pits. Dependent on the chemistry of the intermetallic precipitates, the surrounding aluminum matrix is either cathodic ( $\text{MgZn}_2$ ,  $\text{Mg}_2\text{Si}$ ) or anodic ( $\text{Al}_7\text{Cu}_2\text{Fe}$ ,  $\text{Al}_3\text{Fe}$ ,  $\text{Al}_2\text{CuMg}$ ) to the specific precipitate, leading to preferential corrosion of the matrix (anodic matrix) or precipitate (cathodic matrix), respectively [16].

While large intermetallic precipitates can initiate the pitting corrosion in the samples formed within the heated forming tools, mainly intergranular corrosion occurred in the samples formed without heating. According to literature, this may be due to the formation of a large number of small precipitates at the grain boundaries, leaving a thin precipitate free zone in the adjacent grains [6]. Similar to the large precipitates, the chemistry of the precipitates determines the electrochemical behavior, namely if the grain boundaries or the surrounding matrix corrode.

## 5 Summary

Sheets of AA7075 aluminum alloy were formed using a novel thermo-mechanical process. After solutionizing, the sheets were formed and quenched simultaneously within tempered forming tools at 24 °C or 350 °C and subsequently aged at 120 °C for 20 h. The effect of different cooling rates caused by the tool temperature was investigated on the mechanical and corrosion behavior in this study.

As forming within heated tools can lead to increased ductility, it has to be considered that the microstructural changes, which result from this thermo-mechanical process, also affect the corrosion behavior. After forming at 350 °C tool temperature pitting

corrosion occurred and damaged the surface heavily compared to light intergranular corrosion after forming at 24 °C tool temperature.

The above-mentioned forming process reveals a high potential for forming of high strength aluminum alloys and allows to adjust desired mechanical properties, depending on the application field. The final mechanical and physical properties can be clearly influenced by the process parameter during forming process. Moreover, better formability, lower spring-back and thermal distortion was observed compared to the traditional cold forming processes. The conducted research is a step towards an understanding of the mechanical and corrosion behavior of components with graded properties produced in a single process, which will be the basis for a clever use of materials in manufacturing and component design.

For components that are formed with segmented tools, each adjusted to different temperatures, graded mechanical and corrosion properties are expected from the heated to the non-heated segments as well as intermediate properties that occur from other temperatures between the individual segments. Therefore, the next steps are to investigate the mechanical and corrosion properties of sheets at other temperature steps and later, such components manufactured to have graded properties.

## Acknowledgements

The author would like to thank the Hessen State Ministry for Higher Education, Research and the Arts – Initiative for the Development of Scientific and Economic Excellence (LOEWE) for the financial support of the special research project “ALLEGRO”.

Open access funding enabled and organized by Projekt DEAL.

## 6 References

- [1] M. Tisza, I. Czinege, *International Journal of Lightweight Materials and Manufacture* **2018**, *1*, 229.
- [2] M. Merklein, M. Wieland, M. Lechner, S. Bruschi, A. Ghiotti, *J. Mater. Process. Technol.* **2016**, 228, 11.
- [3] A.D. Kotov, A.V. Mikhaylovskaya, M.S. Kishchik, A.A. Tsarkov, S.A. Aksenov, V.K. Portnoy, *J. Alloys Compd.* **2016**, 688, 336.
- [4] T. Maeno, K.-I. Mori, R. Yachi, *CIRP Ann.* **2017**, 66, 269.
- [5] M. Kumar, N. Sotirov, C.M. Chimani, *J. Mater. Process. Technol.* **2014**, 214, 1769.
- [6] W. Huo, L. Hou, Y. Zhang, J. Zhang, *Mater. Sci. Eng. A.* **2016**, 675, 44.
- [7] J. Lin, T. Dean, R.P. Garrett, A.D. Foster, WO 2008/059242A2, **2007**.
- [8] R.P. Garret, J. Lin, T.A. Dean, *Int. J. Plast.* **2005**, 21, 1640.
- [9] L. Wang, M. Strangwood, D. Balint, J. Lin, T. A. Dean, *Mater. Sci. Eng. A.* **2011**, 528, 2648.
- [10] M.S. Mohamed, A.D. Foster, J. Lin, D.S. Balint, T.A. Dean, *International Journal of Machine Tools and Manufacture* **2012**, 53, 27.
- [11] E. Scharifi, R. Knoth, U. Weidig, *Procedia Manufacturing* **2019**, 29, 481.
- [12] S.-J. Yuan, X.-B. Fan, Z.-B. He, *Procedia Eng.* **2014**, 81, 1780.
- [13] P.F. Bariani, S. Bruschi, A. Ghiotti, F. Michieletto, *CIRP Ann.* **2013**, 62, 251.
- [14] M.S. Mohamed, A.D. Foster, J. Lin, D.S. Balint, T.A. Dean, *International Journal of Machine Tools and Manufacture* **2012**, 53, 27.
- [15] F. Ostermann, *Anwendungstechnologie Aluminium: Korrosionsverhalten von Aluminium*, Springer-Verlag Berlin Heidelberg, Berlin, Heidelberg **2007**.
- [16] M.K. Cavanaugh, R.G. Buchheit, N. Birbilis, *Eng. Fract. Mech.* **2009**, 76, 641.
- [17] N. Birbilis, M.K. Cavanaugh, R.G. Buchheit, *Corros. Sci.* **2006**, 48, 4202.
- [18] P.A. Rometsch, Y. Zhang, S. Knight, *Trans. Nonferrous Met. Soc. China* **2014**, 24, 2003.
- [19] A.U. Rao, V. Vasu, M. Govindaraju, K.S. Srinadh, *Trans. Nonferrous Met. Soc. China* **2016**, 26, 1447.
- [20] F. Ostermann, *Anwendungstechnologie Aluminium: Legierungsaufbau, Wärmebehandlung*, Springer-Verlag Berlin Heidelberg, Berlin **2007**.

Received in final form: June 26<sup>th</sup> 2020